

Selective Plasma-Induced Grafting of Polystyrene onto Polyolefin Blends

I. Keen, G. A. George, P. M. Fredericks

Centre for Instrumental and Developmental Chemistry, Queensland University of Technology, G.P.O. Box 2434, Brisbane Qld. 4001, Australia

Received 26 December 2001; accepted 13 July 2002

ABSTRACT: Plasma pretreatment has been used to generate reactive radicals and oxygenated groups on polymer surfaces for graft polymerization. The polymer substrates studied were composed of a polypropylene–polyethylene (PP–PE) copolymer, which was predominantly PP, and also contained blended ethylene–propylene rubber (EPR) as either about 15 or about 60 mol %. A pure PP substrate was also studied for comparison. The grafted polymer was polystyrene (PS). Raman microspectroscopic 2-dimensional map-

ping was used to elucidate the role of crystallinity and EPR in the plasma treatment and graft polymerization process. It was found that the plasma pretreatment favored the EPR component of the substrate and the graft yield was related to the EPR content. Crystallinity seemed to have a much less significant effect on the grafting reaction. © 2003 Wiley Periodicals, Inc. *J Appl Polym Sci* 88: 1643–1652, 2003

Key words: polystyrene; poly(propylene) (PP)

INTRODUCTION

It is well known that plasma treatment may be used to improve polymer surface properties for bondability,^{1,2} wettability,^{1,3} biocompatibility,⁴ and dyeability.⁵ Typically, a plasma gas interacts with the surface of a polymer substrate where modification processes, such as functionalization and ablation, occur depending on the type of plasma gas,^{1–5} plasma-treatment conditions,^{1–5} and nature of the polymer substrate.⁶

Many workers have used plasma treatment to produce reactive radicals and different types of oxygen functional groups, such as C–OH, C–O, and HO–C=O, as well as C–O–OH linkages, for graft polymerization.^{1–4} Graft polymerization allows the production of new polymer surfaces different from the bulk material.¹ These radicals and functional groups act as initiating sites for grafting for otherwise unreactive polymer surfaces.¹ Free radicals can directly initiate the grafting reaction if the polymer is not exposed to an oxygen-containing atmosphere prior to polymerization. However, if the polymer is exposed to air or oxygen after plasma treatment, then graft polymerization is initiated by the thermal decomposition of peroxides.¹

Characterization of plasma-treated and grafted polymer surfaces has been accomplished by the use of

a number of surface-sensitive techniques such as X-ray photoelectron spectroscopy (XPS) and attenuated total reflection–infrared spectroscopy (ATR–IR).¹ Both techniques have proved useful in the elucidation of the different types of oxygenated groups on the polymer surface.

Recently, we reported the use of vibrational microspectroscopy, both Raman and ATR–IR, by point mapping, to characterize plasma-treated and grafted polymer surfaces.⁷ Both techniques were useful; however, oxygen-containing functional groups on the surface were difficult to detect and quantify by Raman microspectroscopy because this technique is relatively insensitive to polar groups.

Two-dimensional Raman mapping is achieved by collecting spectra in a grid pattern on a selected part of the sample surface by moving the sample under computer control. Characteristics of the sample are determined from measurements of the intensity or area of relevant Raman bands in each spectrum. These are plotted against the spatial position of each spectrum in the spectral series to yield the two-dimensional map. In addition to our previous work, Raman mapping by point illumination has also been used to study the molecular and lamellar orientation of α - and β -trans-crystalline layers of polypropylene and PET composites⁸ and the distribution of different blends in heterogeneous polymer systems⁹ and to achieve amplification of photooxidized sites.¹⁰

Polypropylene (PP) is a widely used polymer because it is inexpensive, lightweight, and has excellent mechanical and electrical properties.¹¹ However, at

Correspondence to: P. M. Fredericks.

low temperatures below its glass transition temperature, PP suffers from embrittlement.¹² Blending PP with a variety of polyolefin rubbers, such as ethylene-propylene rubber (EPR), has proven to improve PP toughness.¹²⁻¹⁸ The rubber particles are dispersed in the PP matrix, acting as a craze barrier and hindering the formation and development of failure cracks during impact. The rubber content, rubber domain size, and distribution of EPR within the PP matrix have been studied.¹²⁻¹⁸ In addition, the effect of EPR on the crystallinity and morphology in the blend has been investigated using many analytical techniques such as scanning electron microscopy (SEM), ¹³C-nuclear magnetic resonance (NMR), optical microscopy, Fourier transform infrared (FTIR), and atomic force microscopy (AFM).¹²⁻¹⁸

The purpose of the work reported here was to study the effect of plasma treatment and grafting of polystyrene (PS) on pure PP and with blended PP/EPR substrates. The PP/EPR substrates were commercially significant injection-molded materials used as polymer supports for combinatorial chemistry. Plasma-induced graft polymerization offers a novel method of grafting PS onto these polymer supports, which has previously been achieved by γ -irradiation¹⁹ and photoirradiation.²⁰ Raman microspectroscopic mapping was the major tool used to study the effect on the polymer of plasma pretreatment and PS grafting.

EXPERIMENTAL

The pure PP and 15 mol % EPR substrates were Montell PMA6000 and PMA6100, respectively (Montell Polyolefins, Wilmington, DE). The blended 60 mol % EPR substrate was provided by Polymerat Pty. Ltd. (Brisbane, Australia). Raman measurements confirmed the EPR content. For Raman microspectroscopy, the pure PP and 15 mol % EPR substrates were embedded in a resin (Araldite™) which was cured overnight at 60°C. A fresh surface for each polymer was exposed by a sharp scalpel and then polished with increasingly finer grades of emery paper. A part of the surface, shown as a shaded square in Figure 1, was examined in detail by Raman mapping experiments. Sample preparation for the 15 mol % EPR substrate and Raman microspectroscopy procedures were described in detail in a previous report.⁷

The plasma-treatment system employed a tubular glass sample chamber with dimensions 50 × 250 mm (diameter × length) and was powered by a 27-MHz Megatherm radio-frequency generator. Full details of the plasma system were given elsewhere.²¹ Prior to treatments, the discharge chamber was tuned for minimum reflected power with a dummy sample on a sample holder in place under the desired reaction conditions of gas and pressure. No measurement was

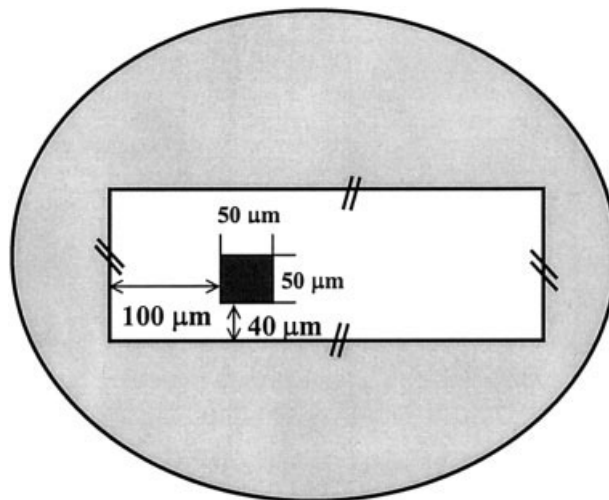


Figure 1 Diagram showing the area of detailed study (black) on the polymer surface (white) embedded in a resin (shaded).

made of the gas flowrate. When this procedure was satisfactory, the sample was inserted and the system was evacuated to 0.01 mTorr. Argon gas was then bled into the chamber to a static pressure of 200 mTorr for 5 min before the plasma was ignited at 20 W for 20 s. After ignition, the chamber was isolated and oxygen gas was allowed into the system to 1 atm for 120 s.

The plasma-treated substrate was grafted with the styrene monomer (Sigma-Aldrich, Sydney, Australia; 99%, with 10–15 ppm of the 4-*tert*-butylcatechol inhibitor) under a nitrogen atmosphere at 70°C for 24 h. After grafting, the substrate was Soxhlet-extracted (to remove monomer and homopolymer) for at least 24 h with dichloromethane and left to dry at room temperature.

RESULTS

Untreated substrates

Figure 2 depicts a portion of the Raman spectra of (a) pure PP, (b) 15 mol % EPR, and (c) 60 mol % EPR. Raman bands at 1064, 1126, 1296, and 1410 cm^{-1} were attributed mainly to the ethylene unit of the EPR component.²² Ethylene units in the PP substrate may also contribute to the intensity of these Raman bands, but this will be small because the ethylene content of the copolymer is known to be small. Generally, the amount of ethylene in the EPR will modify the impact properties of the blend because its glass transition temperature and its adhesion to the PP matrix will be strongly affected.²³

The Raman band at 1064 cm^{-1} may be used for calculating the concentration of the EPR component.⁷ Comparing the two blended substrates, it can be seen that the magnitude of this band increases with an

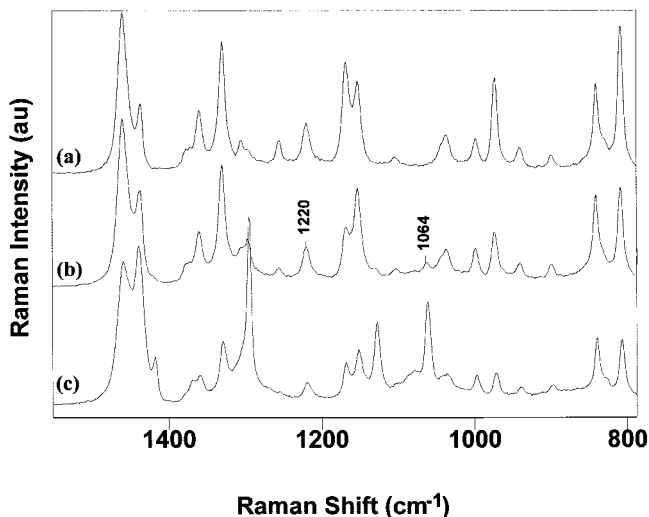


Figure 2 Selected Raman spectra of the polymer substrates: (A) pure PP; (B) 15 mol % EPR/PP; (C) 60 mol % EPR/PP.

increasing amount of EPR. By calculating the integrated area ratio of the bands at 1064 and 1220 cm^{-1} , the proportion of EPR at any point on the surface can be determined. In this way, Raman maps of the distribution of the EPR component for untreated (a) 15% and (b) 60% EPR blend substrates were constructed for the $50 \times 50\text{-}\mu\text{m}$ area under study. These maps are shown in Figure 3. They allow the concentration profile of EPR domains, such as shape and size distribution, across the surface for each sample to be compared at the micrometer level. The Raman map of the 60% EPR substrate showed large areas which were rich in EPR domains so that they coalesced together. In the 15% EPR substrate, however, the Raman map showed a low concentration of EPR across the surface with well-dispersed islands of slightly higher concentration of about $2\text{--}6\text{ }\mu\text{m}$ in size.

PP is a semicrystalline polymer and therefore contains both crystalline and amorphous regions.¹¹ A measure of the crystallinity across the surface of the pure PP and the 15 mol % EPR blend can be determined by taking the area ratio of Raman bands at 998 and 973 cm^{-1} (Fig. 4).²⁴ It can be seen that each surface shows a quite different variation in the surface crystallinity. In the 15 mol % blend [Fig. 4(B)], the surface crystallinity was relatively high and a gradient in crystallinity was apparent across the examined area. For the pure PP substrate [Fig. 4(A)], the surface crystallinity was much lower, but a band of slightly higher crystallinity of about $20\text{ }\mu\text{m}$ wide traversing the surface was also found. The differing crystallinity of the two surfaces could be due to different conditions in the injection-molding process of these substrates, which can affect the degree of crystallinity across the material.²⁵ It should be noted that the Raman signal

does not really originate from only the surface of the polymer, but from a volume shaped somewhat like a truncated ellipsoid which is about $1\text{ }\mu\text{m}$ in diameter at the surface and about $4\text{ }\mu\text{m}$ long.²⁶

The position of the small area of study relative to the faces of the polymer artifact is also important. For example, the bottom section of the 15 mol % blend showed higher crystallinity than that of the rest of the surface. This section is close to the outer face of the substrate which would have been in contact with the mold during the injection-molding process. Hence, the increased crystallinity was probably due to the high shearing forces acting on the polymer as it was forced through the small channels required to injection mold such a small object.²⁷ It was not possible to estimate the crystallinity of the PP matrix in the 60 mol % EPR substrate because the spectra were dominated by bands due to the ethylene units of the EPR.

Plasma-treated substrates

After plasma treatment, Raman maps of the same areas for pure PP and the two blends were obtained. The degree of crystallinity across the surfaces of the (a) pure PP and (b) 15 mol % EPR substrates was replotted. Comparison of these maps (Fig. 5) with those measured before plasma treatment (Fig. 4) shows that plasma treatment has led to a slight decrease in surface crystallinity. Heat generated during plasma treatment is the probable cause of this slight change of surface crystallinity. This result is in contrast with that of Denes et al., who found the surface crystallinity of cellophane substrates to be enhanced after exposure to oxygen plasma.²⁸

To investigate the effect of plasma pretreatment on the EPR, EPR-component Raman maps for both blends were constructed (Fig. 6). It can be clearly seen that, for both EPR-containing substrates, after plasma treatment, there is an increase in the proportion of EPR detected at the surface. Plasma is composed mainly of high-energy charged particles, which can cause damaging processes such as etching and ablation.²⁹ These results show that the PP matrix is more susceptible to ablation than are the EPR domains and segments, thus leaving increased EPR at the surface.

PS-grafted substrates

After grafting, Raman spectra collected for each substrate contained Raman bands attributed to both the grafted PS and the substrate matrix. Evidence of heterogeneous grafting of PS on the surface for all substrates can be displayed by constructing Raman maps by taking the integrated ratio of the PS Raman band near 1600 cm^{-1} to the PP band at 1440 cm^{-1} . These

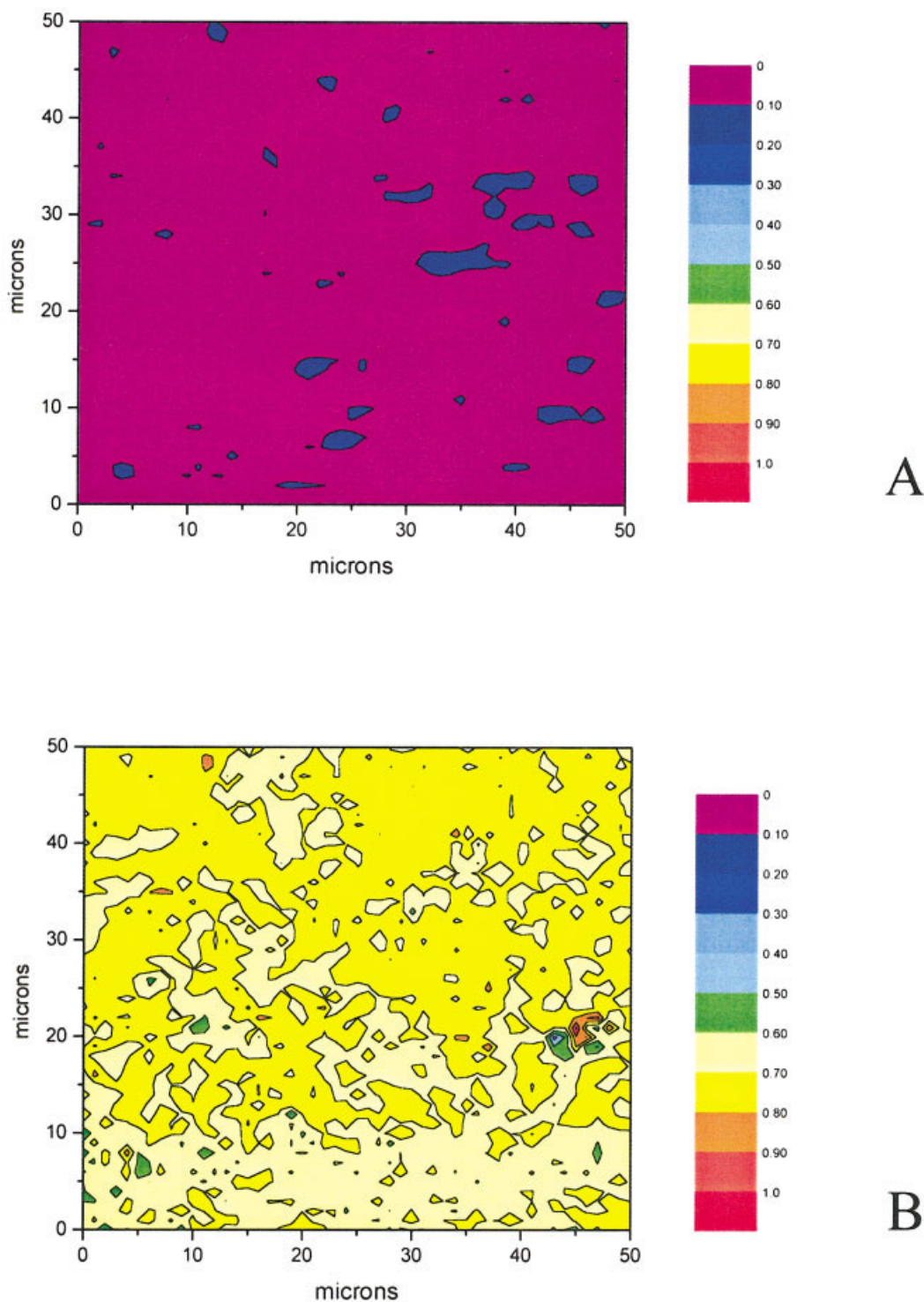


Figure 3 Raman maps showing the surface EPR distribution for the untreated (A) 15 mol % EPR substrate and (B) 60 mol % EPR substrate. [Color figure can be viewed in the online issue, which is available at www.interscience.wiley.com.]

maps (Fig. 7) indicate the distribution of the PS on the surface after grafting.

For the pure PP surface [Fig. 7(A)], the amount of grafting was very low across the whole surface, with a few islands of higher concentration [Fig. 5(A)]. For the

15 mol % EPR substrate [Fig. 7(B)], the area of highest PS grafting corresponded to an area of lower PP crystallinity and higher EPR content on the plasma-treated substrate. It is known³⁰ that the presence of EPR tends to lower the crystallinity of the adjacent PP, so it is

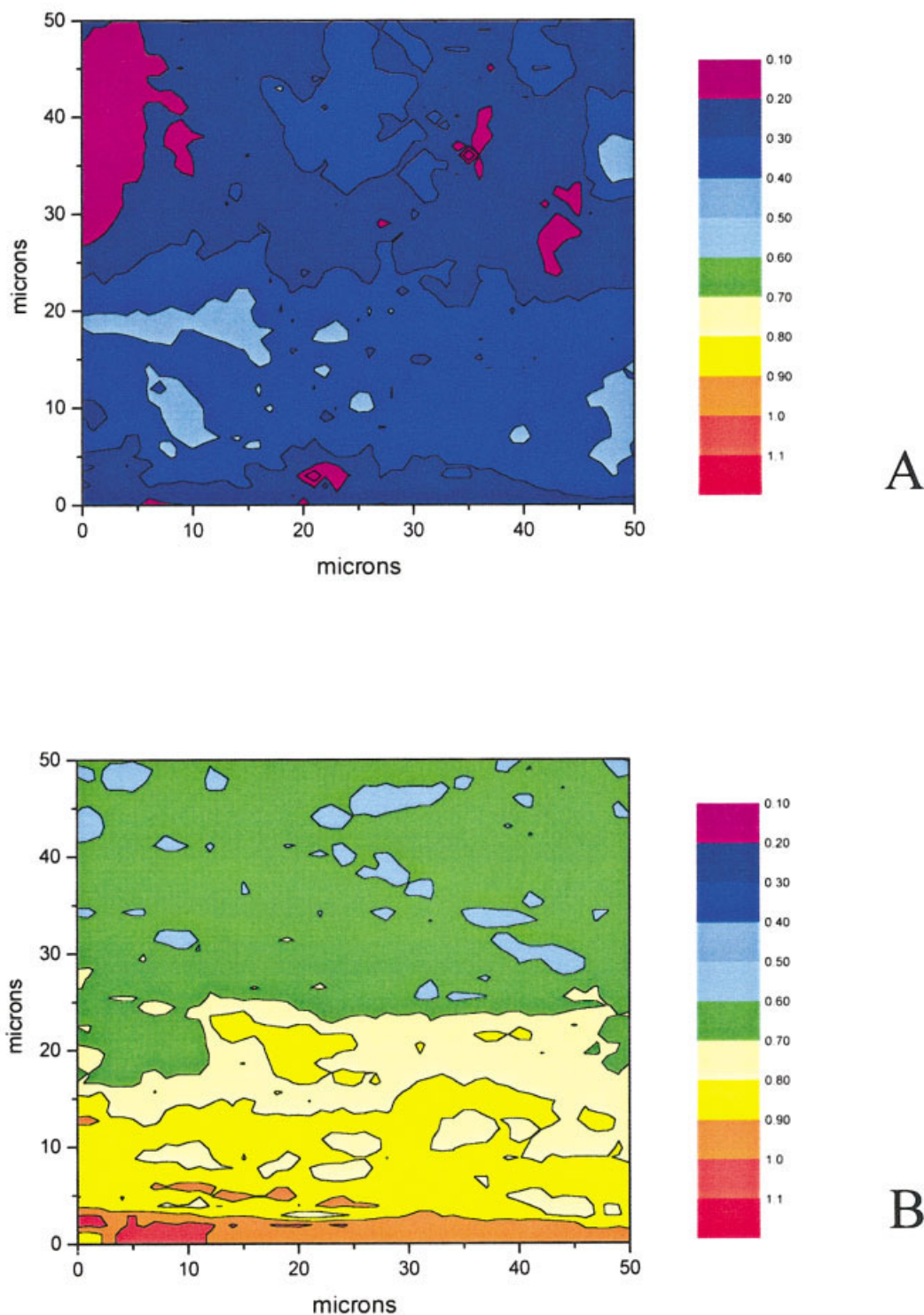


Figure 4 Raman maps showing a measure of the surface crystallinity for the untreated (A) pure PP substrate and (B) 15 mol % EPR substrate. [Color figure can be viewed in the online issue, which is available at www.interscience.wiley.com.]

expected that lower crystallinity and EPR would occur together on the surface. However, it is not immediately apparent whether the important factor for PS grafting is the presence of EPR or the lower PP crystallinity, although the pattern of the PS grafting seems

to correspond to some degree to the pattern of the EPR distribution. This question may be answered by considering the results for the 60 mol % EPR substrate [Fig. 7(C)]. This substrate produced, by far, the highest level of PS grafting and the Raman map shows that the

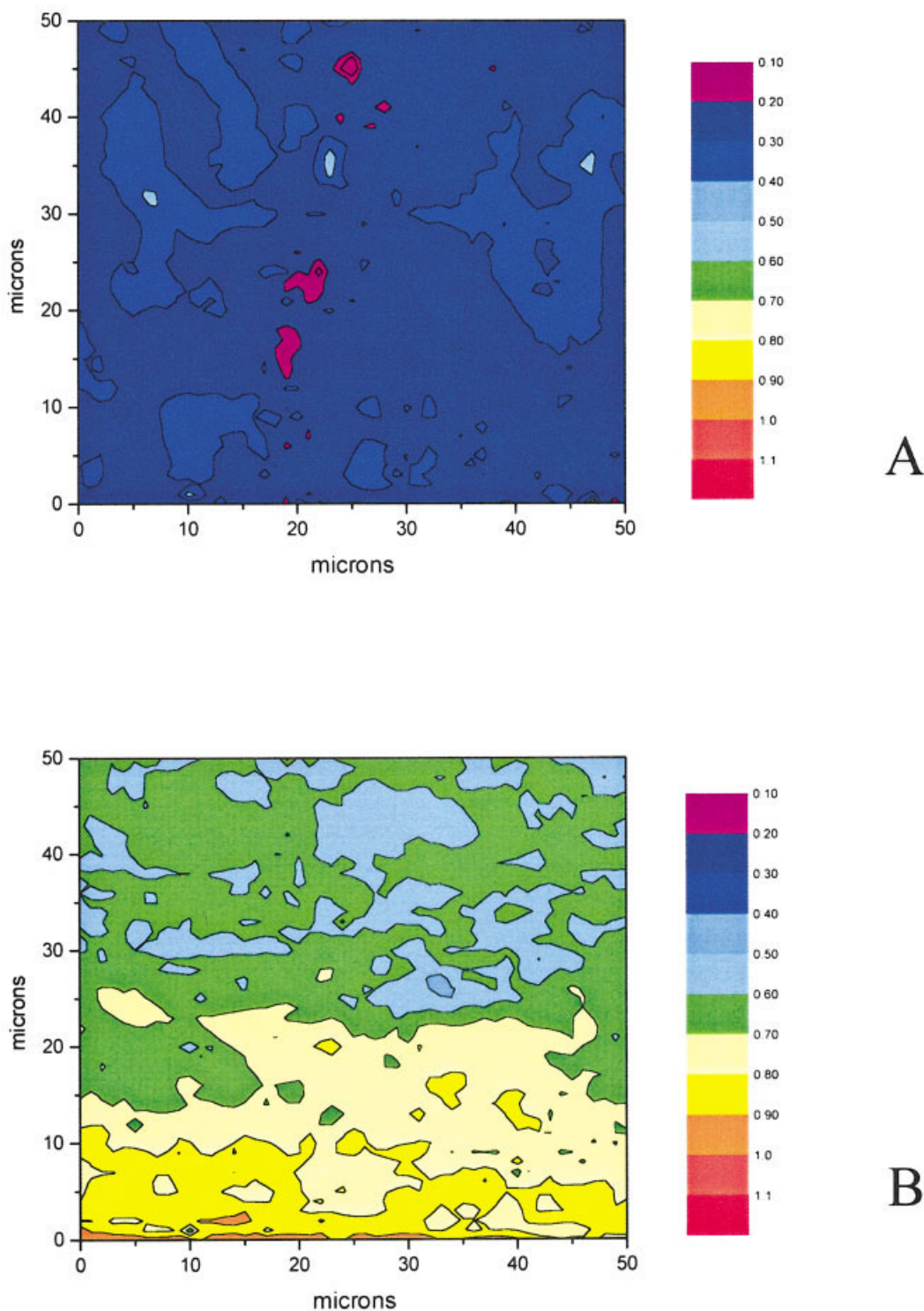


Figure 5 Raman maps showing a measure of the surface crystallinity for (A) the pure PP substrate and (B) the 15 mol % EPR substrate, after plasma treatment. [Color figure can be viewed in the online issue, which is available at www.interscience.wiley.com.]

grafts are spread across the whole surface, with the highest grafting taking place in regions which have the highest EPR content after plasma treatment. This confirms conclusively that the PS is selectively grafting onto the EPR component of the blends.

At first sight, this would appear to be a counterintuitive result since one might expect the PP to be more reactive than is the EPR, because of the high number of tertiary hydrogens present in the PP structure. However, recent work by Kamfjord and Stori on the

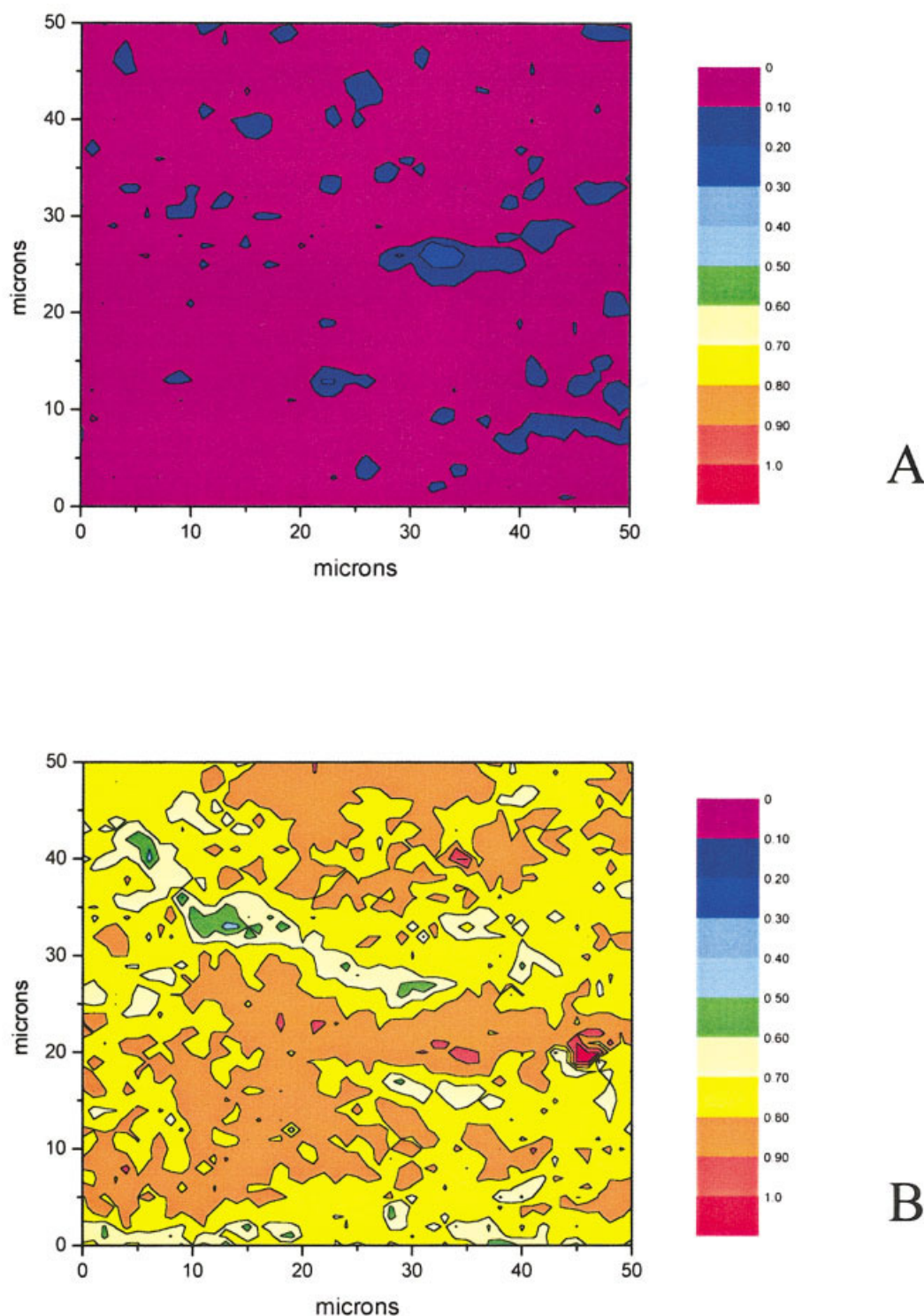


Figure 6 Raman maps showing the surface EPR distribution for (A) the 15 mol % EPR substrate and (B) the 60 mol % EPR substrate, after plasma treatment. [Color figure can be viewed in the online issue, which is available at www.interscience.wiley.com.]

grafting of maleic anhydride (MA) by peroxide-initiated free-radical polymerization onto heterophasic PP showed that grafting occurred preferentially on the ethylene-rich phase.³¹ This was rationalized by sug-

gesting that the adjacent methyl group in PP sterically protects any free radical generated by abstraction of a tertiary hydrogen from attack by the bulky MA. However, the tertiary hydrogens between ethylene units

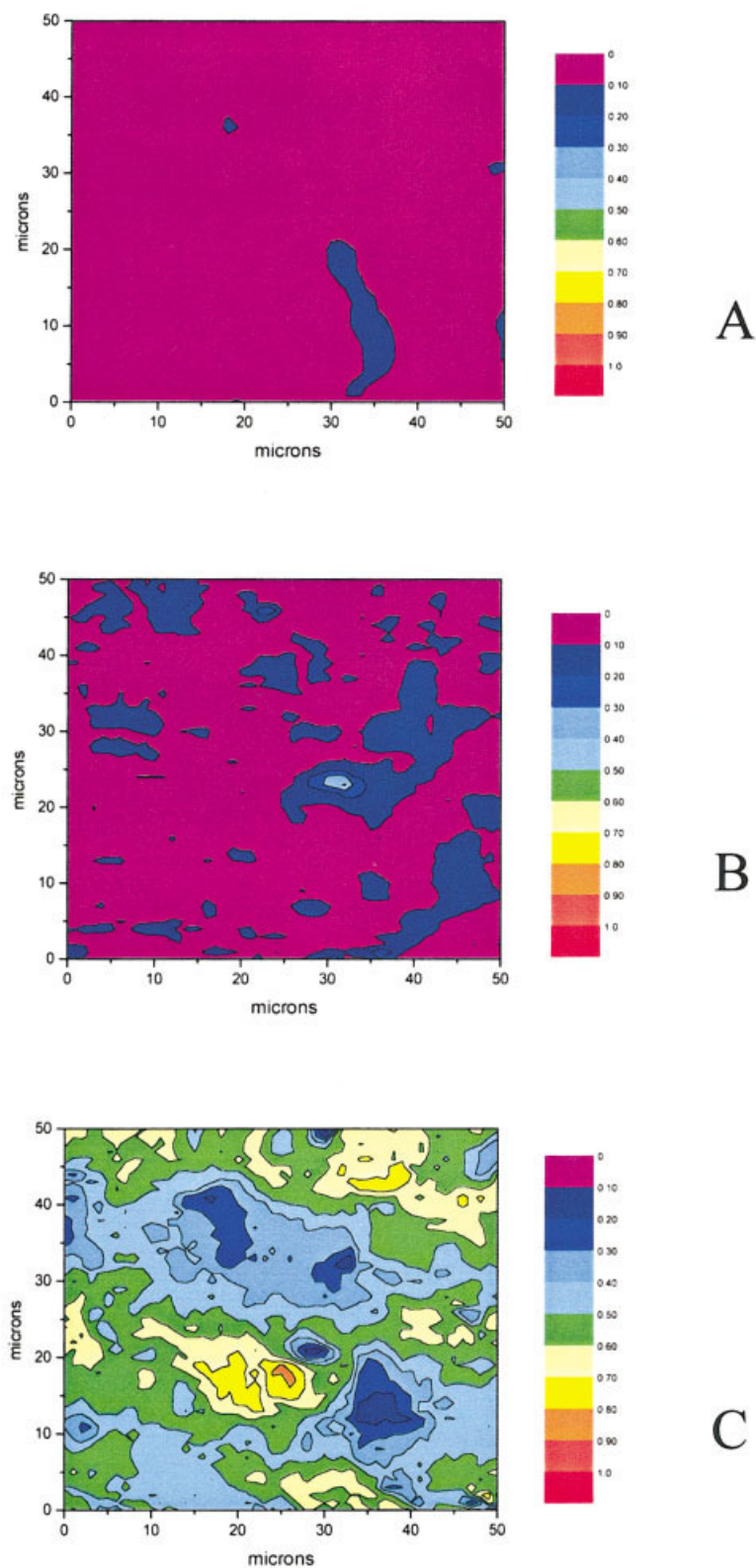


Figure 7 Raman maps showing the distribution of PS on the surface of (A) the pure PP substrate, (B) the 15 mol % substrate, and (C) the 60 mol % substrate, after grafting. [Color figure can be viewed in the online issue, which is available at www.interscience.wiley.com.]

and at the end of PP blocks are more accessible to attack and this leads to preferential grafting in the ethylene-rich phase. Machado et al. also reported a similar result when grafting MA onto a series of polyolefins with different ethylene/propylene ratios.³² They found that the MA graft yield was low for polyolefins with a high propylene content and increased as the ethylene content increased. In particular, they noted that EPR with a propylene content of 50% or less did not display intermediate behavior between PP and polyethylene (PE), but behaved more like PE.

In our case, the exact composition of the EPR component was not known, but we know from the Raman spectrum that it is predominantly composed of ethylene units or we would not have been able to distinguish it so readily from the PP copolymer matrix which was predominantly propylene units.⁷ It therefore appears that the ethylene-rich phase is more susceptible to attack by the plasma, compared with the propylene-rich phase, in the same way as was found by other workers for peroxide-induced grafting. It has been noted³³ that thermoplastic elastomers, such as EPR, are much more susceptible to photooxidation than are other polyolefins due to the totally amorphous nature of the EPR. As a significant component of the argon plasma is higher-energy UV radiation, it may be concluded that the presence of the styrene graft in the same position as the EPR domains reflects the high local concentration of hydroperoxide groups in the amorphous region which are the initiation sites for the PS grafting. While this apparently coincides with regions of higher relative ethylene group concentration, there is no evidence as to whether the actual oxidation sites are the tertiary carbon of the PP or the secondary carbon of PE. The amorphous nature of the EPR plays a role in the chemistry of both the formation of hydroperoxides and their reactions during grafting.

While steric effects in the PP, and the amorphous nature of the EPR, may be contributing factors, if we consider the potential outcome of the radical chemistry, the most probable reason for the selective grafting onto the EPR is the depolymerization of the PP by chain scission during the plasma treatment. PP is known to undergo chain scission, whereas under similar conditions, PE, and, hence, EPR, is more likely to crosslink. This would explain the preferential loss of PP by ablation during plasma treatment, leading to a small increase in the proportion of EPR at the surface. Loss of PP by depolymerization is likely to lead to fewer active sites on the remaining PP surface compared with the EPR which has not depolymerized.

CONCLUSIONS

Raman mapping proved to be an excellent technique to elucidate the role of crystallinity and EPR in the

plasma treatment and graft polymerization process. In addition, investigating exactly the same area after plasma treatment, and subsequently after graft polymerization, offers a method for monitoring the effect of plasma pretreatment and grafting.

For the untreated pure PP and 15 mol % EPR samples, it was shown that different injection-molding process conditions impart a different variation of crystallinity across the substrate. The 15 mol % EPR blend showed a gradient in the crystallinity from the edge into the bulk material. This could be due to the shearing action on the polymer as it was extruded through the mold during the injection-molding process. PP crystallinity could not be measured on the 60 mol % EPR substrate. After plasma treatment, the heating effect of the plasma caused a slight decrease of surface PP crystallinity for pure PP and 15 mol % EPR substrates.

Raman maps of the EPR component for untreated substrates showed different sizes and shapes of EPR domains. In the 60 mol % EPR blend, domains were large and were coalesced, whereas in the 15 mol % EPR blend, only a few island-type domains were present. After plasma treatment, ablation of the PP matrix led to the appearance of slightly more EPR on the surfaces of the blends. After grafting, areas with higher EPR contents corresponded to areas of higher grafted PS. The grafting yield for the pure PP substrate was very low. The results indicate that the ethylene-rich regions of the substrate (i.e., the EPR domains) are more susceptible to attack by the plasma, leading to the generation of oxygen functionality on the surface leading to higher PS grafting yields. The most probable reason for this is the depolymerization of the surface PP by chain scission during argon plasma treatment, leading to fewer active sites compared to the EPR, which is less susceptible to chain scission. Depolymerization also explains the loss of PP by ablation observed during plasma treatment.

The authors thank Dr. Llewellyn Rintoul for his help in acquiring the Raman maps. The authors are also grateful to Dr. Firas Rasoul and Dr. Joe Maeji of Polymerat Pty. Ltd. for supplying samples and for helpful discussions.

References

1. Chan, C.-M. *Polymer Surface Modification and Characterisation*; Hanser/Garner: Cincinnati, 1993.
2. Egitto, F.; Matienzo, L. *IBM J Res Dev* 1994, 38, 423.
3. Zubaidi; T. Hirotsu, *J Appl Polym Sci* 1996, 61, 1579.
4. Feijen, J.; Engbers, G.; Terlingen, J.; Lens, J. *J Biomater Sci Polym Ed* 1998, 9, 357.
5. Rochery, M.; Lam, T. M. *Macromol Symp* 1997, 119, 277.
6. France, R.; Short, R. *Langmuir* 1998, 14, 4827.
7. Keen, I.; Rintoul, L.; Fredericks, P. M. *Appl Spectrosc* 2001, 55, 984.
8. Fernández, M. R.; Merino, J. C.; Gobernado-Mitre, M. I.; Pastor, J. M. *Appl Spectrosc* 2000, 54, 1105.

9. Markwort, L.; Kip, B.; Da Silva, E.; Roussel, B. *Appl Spectrosc* 1995, 49, 1411.
10. Liu, H.; Keen, I.; Rintoul, L.; George, G. *Polym Degrad Stab* 2001, 72, 543.
11. Karger-Kocsis, J. In *Polypropylene. An A-Z Reference*; Karger-Kocsis, J., Ed.; Kluwer: Dordrecht, 1999; p 8.
12. Utracki, L. A. In *Polypropylene. An A-Z Reference*; Karger-Kocsis, J., Ed.; Kluwer: Dordrecht, 1999; p 621.
13. Mehrabzadeh, M.; Hossein Nia, K. *J Appl Polym Sci* 1999, 72, 1257.
14. Hongjun, C.; Xiaolie, L.; Dezhu, M.; Jianmin, W.; Hongheng, T. *J Appl Polym Sci* 1999, 71, 93.
15. Feng, Y.; Hay, J. N. *Polymer* 1998, 39, 6723.
16. Pennington, B. D.; Ryntz, R. A.; Urban, M. W. *Polymer* 1999, 40, 4795.
17. D'Orazio, L.; Cecchin, G. *Polymer* 2001, 42, 2675.
18. Tomasetti, E.; Legras, R.; Nysten, B. *Nanotechnology* 1998, 9, 305.
19. Nho, Y. C.; Chen, J.; Jin, J. H. *Radiat Phys Chem* 1999, 54, 317.
20. Li, Y.; Desimone, J.; Poon, C.-D.; Samulski, E. T. *J Appl Polym Sci* 1997, 64, 883.
21. George, G. A.; Cash, G. A.; Le, T. T.; Goss, B. A. S.; Wood, B. J.; Brown, J. R.; St. John, N. A. *Polym Adv Technol* 1995, 7, 343.
22. Bower, D. I.; Maddams, W. F. *The Vibrational Spectroscopy of Polymers*; Cambridge University: Cambridge, England 1989.
23. Costa, J. L. In *Polypropylene. An A-Z Reference*; Karger-Kocsis, J., Ed.; Kluwer: Dordrecht, 1999; p 503.
24. Andreassen, E. In *Polypropylene. An A-Z Reference*; Karger-Kocsis, J., Ed.; Kluwer: Dordrecht, 1999; p 320.
25. Minardi, A.; Boudeulle, M.; Duval, E.; Etienne, S. *Polymer* 1997, 38, 3957.
26. Keen, I.; Rintoul, L.; Fredericks, P. M. *Macromol Symp* 2002, 184, 287.
27. Bryce, D. M. *Plastic Injection Molding—Material Selection and Product Design Fundamentals*; Society of Manufacturing Engineers: Dearborn, MI, 1997.
28. Denes, F.; Sitaru, R.; Young, R. A. *J Photopolym Sci Tech* 1998, 11, 299.
29. Mühlhan, C.; Nowack, H. *Surf Coat Technol* 1998, 98, 1107.
30. Yokoyama, Y.; Ricco, T. *J Appl Polym Sci* 1997, 66, 1007.
31. Kamfjord, T.; Stori, Aa. *Polymer* 2001, 42, 2767.
32. Machado, A. V.; Covas, J. A.; van Duin, M. *Polymer* 2001, 42, 3649.
33. Zweifel, H. *Stabilization of Polymeric Materials*; Springer-Verlag: Berlin, 1998.